Voltage Sag Effects on High Performance Electric Drives

M. Petronijević, N. Mitrović, and V. Kostić

***Abstract*—This paper researches symmetrical and unsymmetrical voltage sag influence on speed and torque deviation in rotor field oriented (RFO) and direct torque controlled (DTC) drives. To overcome appeared drop in speed and torque ripple it was proposed a field-weakening algorithm during voltage sag and/or disturbance estimator application in torque control loop. Prompt DTC flux recall enables efficiency overcoming torque deviation.**

***Index Terms*—Voltage sag, field orinted control, direct torque control, torque ripple, power quality.**

I. Introduction

FREQUENCY converters present sophisticated and nonlinear power electronics devices, which are used in manifold industry branches, in wide range of installed power. Mainly, these AC voltage converters consist of input rectifier (in most cases three-phase diode bridge), DC link circuit, output converter (three-phase inverter with power switching transistors) and additional system for protection, measuring and control. Each of the mentioned subsystem can particularly respond in case of power supply disturbance appearing or in coupling with other sub systems. Complex converter sensitivity of power quality parameters are achieved as a unique response of the overall subsystems.

Frequency converters voltage sag sensitivity is led by various studies and experimental researches (e.g. [1]), in which determined sensitivity limits for equipment operation is related only to disconnection/tripping. Voltage sags may cause significant adjustable speed drives performance degradation: symmetrical voltage sags lead to maximum available torque reduction ([2]) and unsymmetrical ones consequently initiate DC link voltage ripple. Problem of the influence of unsymmetrical voltage sags on adjustable speed drives was analytically examined in [3] and [4] where the importance of specific DC bus capacitance value (μF/kW) is stressed. Reference [5] presents some experimental results referring to unsymmetrical voltage sag influence and recommends under voltage protection settings to overcome power quality disturbance.

Recently researches in voltage sags sensitivity have not taken into consideration control algorithm influence in order to maintain operation without loss of performance. This paper experimentally verifies control algorithms influence on symmetrical (type A) and unsymmetrical (type B) voltage sags outcomes, especially in high performance electric drives. In case of an input supply voltage reduction, which does not trigger under voltage protection, usual converter control brings along torque reduction, meanwhile to the drop in speed. Based on analytical relation and detailed computer simulation we presented the new method, which overcome conventional control method limits. The algorithm was successfully tested on dSpace prototyping system DS1104 applied in electric drives with rotor field oriented control (RFOC) and direct torque and flux control (DTC).

Unsymmetrical voltage sags B, C, and D types are the results of the most common fault – single-phase short circuit ([6]). Numerous sags of the previous mentioned types (over 70% of all sags in network) and the fact that DC bus voltage usually remains over undervoltage protection limit provoke the idea of undesired torque ripple elimination.

In case of RFOC induction motor drive, it was proposed internal current control loop modification by adding a disturbance observer. It was revealed that DTC drives are less sensitive to this sag type, even in case of modified control method with constant switching frequency and PI (proportional–integral) flux and torque controller. Experimental results follow up achieved results and present the applied methods effectiveness for disturbance elimination.

II. RFO and DTC Induction Motor Drives

Nowadays, two basic industrial solutions are designated as methods of instant torque control in high performance induction motor drives:

- **Vector control:** based upon stator currents control in synchronous reference frame, using pulse width modulation (PWM);
- **Direct torque control:** based upon stator flux phasor position control, in the basic method with hysteresis controllers for stator flux magnitude and instantaneous torque value.

Basic control structure, which uses indirect rotor field orientation control (IFOC), was shown in Fig. 1. Two inner current control loops for d and q stator currents component are noted and synchronous speed (ω_e) estimator based on

M. Petronijević, N. Mitrović, and V. Kostić are with the Faculty of Electronic Engineering, University of Niš, Niš, Serbia.

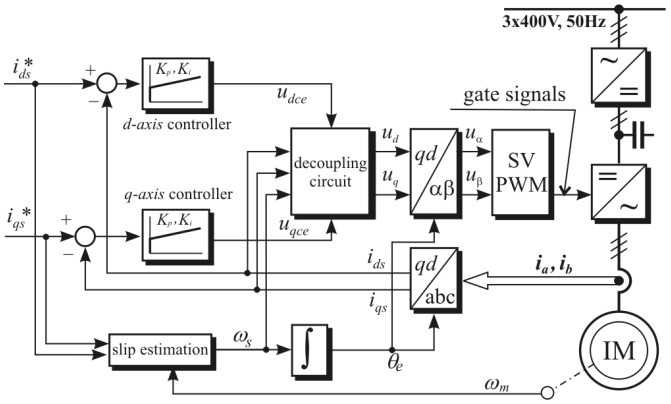

Fig. 1. Basic IFOC control scheme.

reference stator currents components. Linear PI controllers are mainly used. Basic equations for proportional (K_p) and integral (K_i) gain adjusting for q and d current loops, considering decoupling circuit influence, are shown in [7]. In the experiments accomplished in this paper, currents control loops bandwidth is set on 1250rad/s, which is a consequence of noise presence in measured currents. For induction motor data given in Table I digital PI controllers for d and q loops are with

TABLE I
MOTOR DATA (PER PHASE) AND LIST OF USED SYMBOLS

Symbol	Motor data
R_s	Stator resistance, 2.7 Ω
R_r	Rotor resistance, 2.22 Ω
L_{ls}, L_{lr}	Stator and rotor leakage inductance, 10.5mH
L_m	Mutual inductance, 0.27 H
u_{sd}, u_{sq}	d and q axis stator voltages
i_{sd}, i_{sq}	d and q axis stator currents
i_{rd}, i_{rq}	d and q axis rotor currents
P	Pole pairs, 1
P_n	Induction motor rated power, 2200W
U_n	Public distribution network rated voltage, 400V
ω_n	Angular rated speed, 297 rad/s
σ	Leakage coefficient, 0.0733
T_r	Rotor time constant, 0.126s
m	Modulation index

K_p=21.75 and K_i=0.768 when sample time is 100μs.

Adequate current control loop adjusting is presented in Fig. 2. where in torque control regime (pulse torque train reference ±2.5Nm) is speed response presented.

In the simplest variant direct torque control, consist of three level hysteresis comparator for torque control and two-level hysteresis comparator for flux. To achieved the acceptable torque ripple it is necessary to calculate appropriate switching states executing in time which is about 10 times shorter (≈25μs) then switching frequency. The same hardware

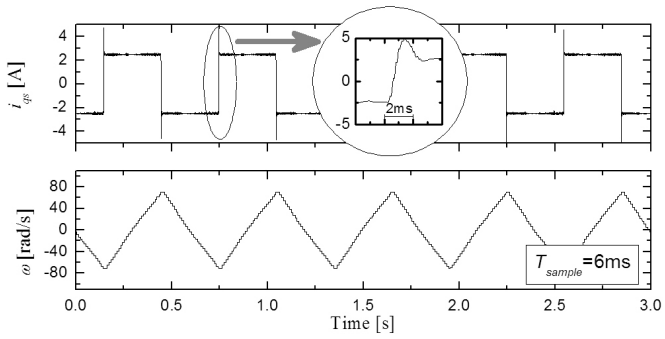

Fig. 2. IFOC drive dynamic performance (top – estimated torque T_e [Nm], bottom – speed ω_m [rad/s]).

prototype platform usage needed modified DTC method realization with PI torque and flux controllers with identical sample and calculation time as in IFOC control algorithm. Basic modified control structure (PI-DTC) was shown in Fig. 3. Constant switching frequency was realized by space vector PWM (SV-PWM). Initial PI controllers' parameters adjusting are accomplished by symmetric optimum method given in [9]. During the experiment parameters where additionally adjusted to achieve torque control loop bandwidth equal to 1250rad/s, which is the same with IFOC current control loops bandwidths.

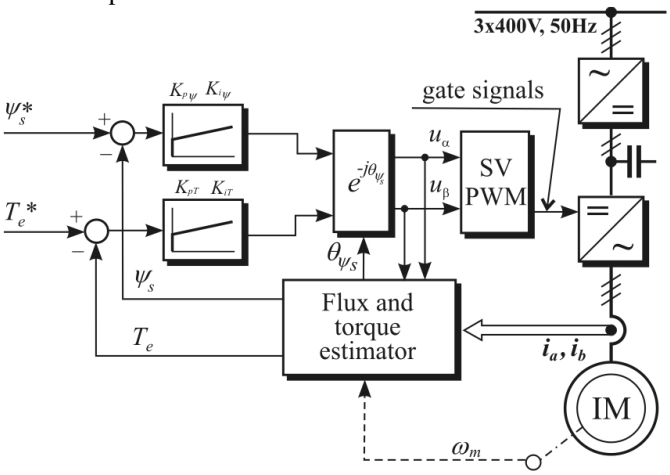

Fig. 3. Modified PI-DTC control scheme.

Illustration of dynamical performances of DTC drives is shown on Fig. 4 with identical control requirements as for IFOC.

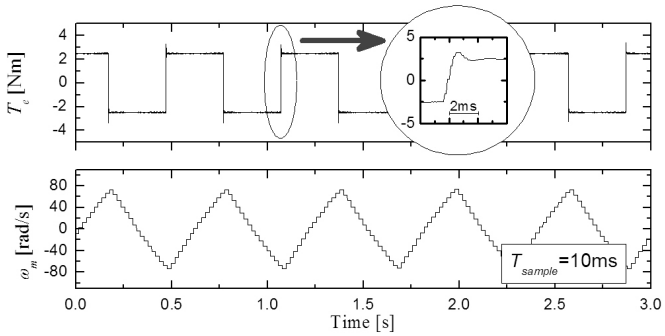

Fig. 4. PI-DTC drive dynamic performance (top – estimated torque T_e [Nm], bottom – speed ω_m [rad/s]).

III. SYMMETRICAL VOLTAGE SAG EFFECTS

Under the assumptions of linear magnetic circuit and balanced operating conditions, induction motor can be described by the following set of equations in two-phase synchronous reference frame:

$$\begin{bmatrix} u_{ds} \\ u_{qs} \end{bmatrix} = \begin{bmatrix} R_s & 0 \\ 0 & R_s \end{bmatrix} \begin{bmatrix} i_{ds} \\ i_{qs} \end{bmatrix} + \begin{bmatrix} p & -\omega_s \\ \omega_s & p \end{bmatrix} \begin{bmatrix} \lambda_{ds} \\ \lambda_{qs} \end{bmatrix} \quad (1)$$

$$\begin{bmatrix} 0 \\ 0 \end{bmatrix} = \begin{bmatrix} R_r & 0 \\ 0 & R_r \end{bmatrix} \begin{bmatrix} i_{dr} \\ i_{qr} \end{bmatrix} + \begin{bmatrix} p & -\omega_r \\ \omega_r & p \end{bmatrix} \begin{bmatrix} \lambda_{dr} \\ \lambda_{qr} \end{bmatrix} \quad (2)$$

In the previous equation p represents the differential operator, ω_r - slip angular velocity ($\omega_r = \omega_s - \omega$), ω_s - synchronous reference frame speed and ω is rotor angular speed ($\omega = P\omega_m$).

Basic equations for flux linkage are:

$$\begin{aligned} \lambda_{ds} &= L_s i_{ds} + L_m i_{dr}, \ \lambda_{qs} = L_s i_{qs} + L_m i_{qr} \\ \lambda_{dr} &= L_r i_{dr} + L_m i_{ds}, \ \lambda_{qr} = L_r i_{qr} + L_m i_{qs} \end{aligned} . \quad (3)$$

Electromagnetic torque can be calculated by using the following formula:

$$T_e = \frac{3}{2} P \frac{L_m}{L_r} (i_{qs}\lambda_{dr} - i_{ds}\lambda_{qr}) . \quad (4)$$

If the reference frame d-axis is aligned with rotor flux linkage phasor (this presumption does not determine control method), the flux component will be:

$$\lambda_{qr} = 0, \lambda_{dr} = \lambda_r . \quad (5)$$

Limits as consequences of the maximum converter output current (I_{max}) and the maximum PWM voltage at motor stator terminals (U_{max}) referring to appropriate qd motor quantities can be written:

$$i_{qs}^2 + i_{ds}^2 \le I_{\max}^2 \quad \text{(current limit)} \quad (6)$$

$$u_{qs}^2 + u_{ds}^2 \le U_{\max}^2 \quad \text{(voltage limit).} \quad (7)$$

Voltage limit equation, respecting the presumption (5) and basic motor equation, is transformed to:

$$A i_{ds}^2 + C i_{qs}^2 + B i_{ds} i_{qs} \le U_{\max}^2 \quad (8)$$

where: $A = R_s^2 + \omega_s^2 L_s^2$; $B = 2R_s\omega_s \frac{L_m^2}{L_r}$ and $C = R_s^2 + \omega_s^2 \sigma^2 L_s^2$.

If we suppose that IFOC drive operation in basic speed range is with constant rotor flux, reference d-axis stator current at steady state will be:

$$i_{ds}^* = \lambda_r / L_m \quad (9)$$

Equations (6), (8) and (9) represent IFOC drive static characteristics during voltage sag operation and presented in dq reference frame in Fig. 5.

DTC drive posses a control requirement to remain constant stator flux magnitude in basic speed range. Because of this d stator current component will be:

$$i_{ds} = \sqrt{(\lambda_s^*)^2 - \sigma^2 \cdot L_s^2 \cdot i_{qs}^2} / L_s . \quad (10)$$

The last formula accompanied by current (6) and voltage (8) limit equations explains DTC drive steady state characteristics

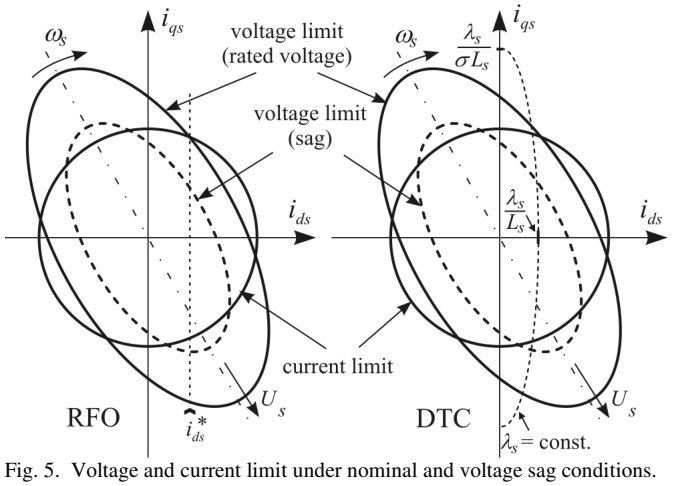

Fig. 5. Voltage and current limit under nominal and voltage sag conditions.

in voltage drop regime, which is also shown in Fig. 5. Obvious fact is that IFOC and DTC drive control differences can lead to various torque limits during voltage sag conditions.

Maximum output PWM voltage reduction during voltage sag provokes decreasing of the available electromagnetic torque with the possible consequence of drop in speed and loss of control accuracy. The main idea of the proposed algorithm is to readjust flux reference value to available voltage at motor terminals. More analytical and simulation results can be found in [2]. This paper in chapter 5 only presents IFOC and DTC drive responses in symmetric three-phase voltage sag as an illustration.

Having in mind that rotor flux recall is restrained by rotor time constant T_r influence it is necessary to enhance stator current component i_{ds} to prevent droop in speed. DTC drive reference flux λ_s^* prompt recall does not require to enhance flux-producing component.

IV. UNSYMMETRICAL VOLTAGE SAGS EFFECTS

Voltage sags B, or C and D types influence input rectifier to be transformed into single-phase operation having as a consequences input current distortion, and DC bus voltage ripple increasing with 100Hz dominant component [3]. Output inverter, properly controlled, transforms DC bus voltage to PWM voltage, which is applied at motor stator terminals.

Modulation signals are generally presented as:

$$u_i(t) = u_i^*(t) + e_i(t) \quad (11)$$

where $e_i(t)$ are injected harmonics (also represents direct transformation SVPWM into carrier based PWM [10]), and $u_i^*(t)$ are called fundamental signals. Fundamental components of line to neutral output PWM voltages are:

$$u_{an}(t) = \frac{1}{2} v_{dc}(t) \cdot [\overbrace{m \cdot \sin(\omega_{out} t + \varphi)}^{u_{ai}^*} + e_i(t)]$$

$$u_{bn}(t) = \frac{1}{2} v_{dc}(t) \cdot [m \cdot \sin(\omega_{out} t + \frac{2\pi}{3} + \varphi) + e_i(t)]$$

$$u_{cn}(t)=\frac{1}{2}v_{dc}(t)\cdot[m\cdot\sin(\omega_{out}t+\frac{4\pi}{3}+\varphi)+e_i(t)] \qquad (12)$$

where ω_{out} - inverter output fundamental frequency with modulation index *m*. Phase angle φ corresponds to initial phase voltage angle respecting to *d* axis. DC bus voltage $v_{dc}(t)$ in single-phase operation having in mind [3] can be written as:

$$v_{dc}(t)=V_{DC}+V_{DC2}\cos(2\omega_i t+\theta_2) \qquad (13)$$

where V_{DC} presents DC voltage mean value, V_{DC2} is second harmonic voltage amplitude, ω_i is power supply frequency ($2\pi 50$ s^{-1} or $2\pi 60$ s^{-1}) and θ_2 is second harmonic angle regarding to reference *d*-axis which defines points on wave at the sag initiation.

Combining equations (12) and (13), and applying coordinate transformations induction motor stator voltages in *dq* reference frame are:

$$u_{ds}(t)=\frac{1}{2}mV_{DC}\sin\varphi+\frac{1}{2}mV_{DC2}\cos(2\omega_i t+\theta_2)\sin\varphi$$

$$u_{qs}(t)=\frac{1}{2}m_1V_{DC}\cos\varphi+\frac{1}{2}m_1V_{DC2}\cos(2\omega_i t+\theta_2)\cos\varphi\,. \qquad (14)$$

In equations above second term is direct consequence DC link voltage ripple because of rectifier single-phase operation. According to [3] sag type, DC link components arrangement and load value influence on voltage pulsation. Having in mind that inverter and motor behave as active load it is hard to calculate second harmonic voltage V_{DC2} value and to predict undesirable torque component value. Beside this, in recent analysis the influence of the fast inner current or torque control loop was not considered.

Combining equations (14) with (1) and (2) and (3) we can, based on (4), calculate in closed form the torque value:

$$T_e=T_{e0}+T_{e2}\cos(2\omega_i t+\phi_2)+T_{e4}\cos(4\omega_i t+\phi_4) \qquad (15)$$

and T_{e0} presents average DC component, T_{e2} is second harmonic amplitude, and T_{e4} is fourth toque harmonic amplitude. More details about calculation can be found in [3], but the achieved results must be accepted carefully, valid only for scalar controlled drives. Illustration from (15) is given in Fig. 6 where single-phase voltage sag consequences are presented. Clearly are noted dominant second harmonics in DC voltage and motor torque. Torque pulsating components can, beside noise increasing, exciting resonance oscillation in mechanically coupling multimotor drives as paper production lines.

In high performance drives, especially in DTC drives, can be expected the undesirable torque pulsation will be significantly suppressed if the inner control loops bandwidth is greater than the dominant second harmonic frequency (100Hz). Usual adjusting of the q-axis stator current component or torque control loops satisfies this requirement. In the next Chapter, we present experimental results regarding to IFOC and DTC drives under single-phase voltage sag.

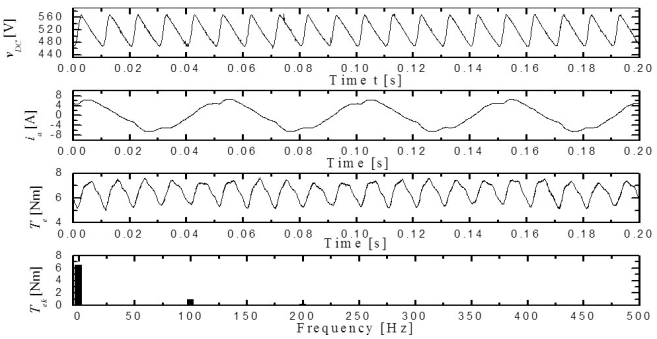

Fig. 6. B type voltage sag effect in drive with V/f control method (load torque= 80% rated, output frequency= 20Hz).

V. Experimental Results

Electric drive control algorithms are implemented by using rapid prototyping system based on dSpace DS1104 control board and Matlab/Simulink software. The experimental verification of the theoretical results was carried out at drive system, which consists of the modified industrial frequency converter, with nominal power of 3.1kVA, an induction motor designated nominal power 2.2kW and a TTL pulse generator with 1024 pulse/revolution was mounted at drive shaft end. Induction motor mechanical loading was done by AC servo drive, which was directly coupled with motor under test. Simple voltage sag generator was made using three-phase power transformer rated power 15kVA with the tap changer under load.

IFOC drive current control subsystem, coordinate transformation blocks, decoupling circuit and slip calculation estimator was realized digitally with the sample time equal to 100μs. Slower speed control loop was implemented with 10ms sample time. Switching frequency of symmetrical SVPWM modulation is set at 5kHz, which also presents simultaneous sampling frequency for two stator currents. In DTC drive torque and flux control loops calculation time period set to 100μs. Sampling time regarding to speed control loop and SVPWM switching frequency are equal to IFOC drive settings.

Fig. 7 illustrates three-phase voltage sag influence for both types of high performance drives. The results of the application enhance of rotor flux readjusting, also stator flux recalls are shown in the same figure. Efficiency of the proposed algorithm in details was discussed in separate paper [2].

To avoid the influence of the speed control loop on torque pulsation we carried out an experiment in torque control regime where rated motor load was applied. At converter terminals we cut off one phase at *t*=0.24s which respond to the B type voltage sag. In Fig. 8, electromagnetic torque time diagram was shown where it could be clearly noted torque pulsation, which is significantly suppressed regarding to *V/f* drive. These torque harmonics also exist at same characteristics frequencies.

One of the simplest methods for this periodic pulsation

reduction is disturbance observer application in current control loop, only for q axis. In Fig. 9 can be seen undesirable torque components reduction.

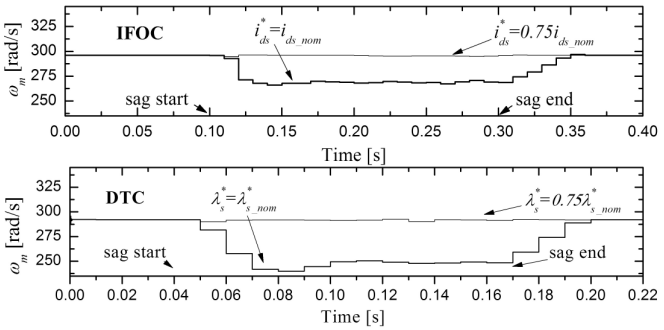

Fig. 7. IFOC (top) and DTC (bottom) drive drop in speed (load torque= 100% rated, U_{sag}=75%U_n).

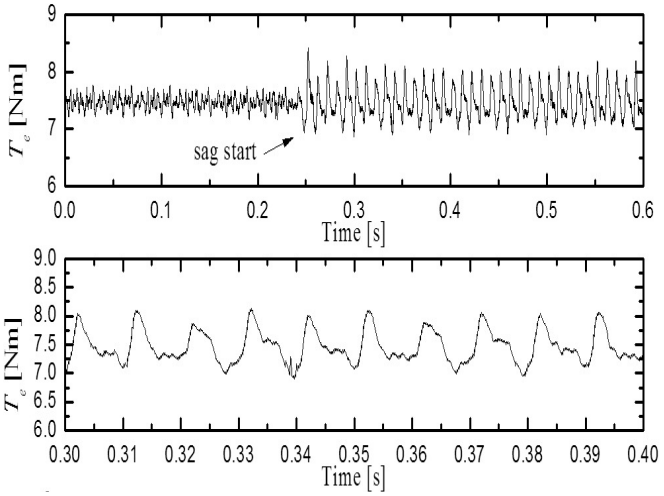

Fig. 8. B type voltage sag effect in drive with IFOC control (load torque= 100% rated).

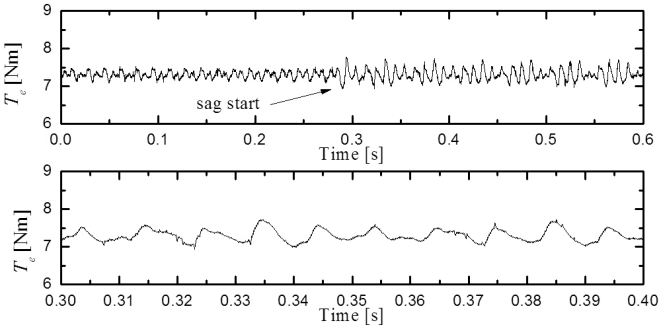

Fig. 9. B type voltage sag effect in drive with IFOC control (load torque= 100% rated, *Q* observer application).

DTC controlled drive was also tested on B type voltage sag which was initiate at time *t*=0.22s. In Fig. 10, it can be seen minor voltage sag sensitivity, which is represented by small additional torque harmonic component.

VI. CONCLUSION

In high performance adjustable speed drives can be expected the undesirable torque pulsation and speed reduction if voltage disturbance occur at input converter terminals.

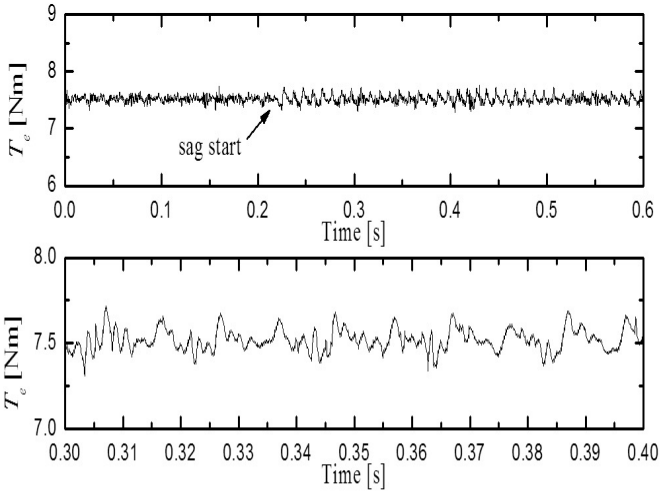

Fig. 10. B type voltage sag effect in drive with DTC control (load torque= 100% rated).

Simplified analysis, without control algorithm taking into account, yields inaccurate results. Numerous simulation and experimental results identifies significant differences in drive behaviors. In high performance drives, especially in DTC drives, can be expected the undesirable torque pulsation will be significantly suppressed. Disturbance observer application in IFOC drives significantly reduces torque pulsation. Further research will be based on application of advanced disturbance estimators. This is significant for converters with lower value of DC link capacitance.

REFERENCES

[1] S. Ž. Djokić, K. Stockman, J. V. Milanović, J.J. M. Desmet, and R. Belmans, "Sensitivity of AC adjustable Speed drives to voltage sags and short interruptions", IEEE Trans. Power Delivery, vol. 20, no. 1, pp. 494–505, Jan. 2005.

[2] Petronijevic, M.P.; Jeftenic, B.I.; Mitrovic, N.M.; Kostic, V.Z., "Voltage sag drop in speed minimization in modern adjustable speed drives," Industrial Electronics, 2005. ISIE 2005. Proceedings of the IEEE International Symposium on , vol.3, pp. 929-934 vol. 3, 20-23 June 2005.

[3] K. Lee, T. M. Jahns, W. E. Berkopec and T. A. Lipo, "Closed-form analysis of adjustable speed drive performance under input voltage unbalance and sag conditions", IEEE Trans. Ind. Appl., vol.42, no.3, May/June, 2006, pp. 733-741.

[4] M. H. J. Bollen, and L. D. Zhang, "Analysis of voltage tolerance of AC adjustable-speed drives for three-phase balanced and unbalanced sags", IEEE Trans. Ind. Appl., vol.36, no.3, May/June, 2000, pp. 904-910.

[5] K. Stockman, F. D'hulster, K. Verhaege, M. Didden, and R. Belmans, "Ride-through of adjustable speed drives during voltage dips" Electric Power System Research, vol 66, pp. 49-58, 2003.

[6] M. H. J. Bollen, Understanding power quality problems: Voltage sags and interruptions, IEEE Press series on Power Engineering, New York, 2000.

[7] D. Telford, M. W. Dunnigan, and B. W. Williams, "Online Identification of Induction Machine Electrical Parameters for Vector Control Loop Tuning," IEEE Trans. Ind. Electron., vol. 50, no. 2, pp. 253-261, April 2003.

[8] Y. S. Lai, and J.H. Chen, "A New Approch to Direct Torque Control of Induction Motor Drives for Constant Inverter Switching Frequency and Torque Ripple Reduction," IEEE Trans. On Energy Conversion, vol.16, no.3, Sept., 2001, pp. 220-227.

[9] M. P. Kazimierkowski, F. Blaabjerg, and R. Krishnan, Control in Power Electronics – Selected problems, Academic Press, New York, 2002.

[10] K. Zhou, and D. Wang, "Relationship between space-vector modulation and three-phase carrier-based PWM: a comprehensive analysis", IEEE Trans. Ind. Electr. vol.49, no.1, February, 2002, pp. 186-196.